

This is an electronic reprint of the original article.

This reprint *may differ* from the original in pagination and typographic detail.

Author(s): Aleksi Isoaho, Lauri Ikkala, Hannu Marttila, Jan Hjort, Timo Kumpula, Pasi Korpelainen & Aleksi Räsänen

Title: Spatial water table level modelling with multi-sensor unmanned aerial vehicle data in boreal aapa mires

Year: 2023

Version: Published version

Copyright: The Author(s) 2023

Rights: CC BY 4.0

Rights url: <http://creativecommons.org/licenses/by/4.0/>

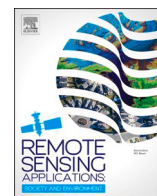
Please cite the original version:

Isoaho, A., Ikkala, L., Marttila, H., Hjort, J., Kumpula, T., Korpelainen, P., & Räsänen, A. (2023). Spatial water table level modelling with multi-sensor unmanned aerial vehicle data in boreal aapa mires. *Remote Sensing Applications: Society and Environment*, 32, 101059.
<https://doi.org/10.1016/j.rsase.2023.101059>

All material supplied via *Jukuri* is protected by copyright and other intellectual property rights. Duplication or sale, in electronic or print form, of any part of the repository collections is prohibited. Making electronic or print copies of the material is permitted only for your own personal use or for educational purposes. For other purposes, this article may be used in accordance with the publisher's terms. There may be differences between this version and the publisher's version. You are advised to cite the publisher's version.

Contents lists available at [ScienceDirect](https://www.sciencedirect.com)

Remote Sensing Applications: Society and Environment

journal homepage: www.elsevier.com/locate/rsase

Spatial water table level modelling with multi-sensor unmanned aerial vehicle data in boreal aapa mires

Aleksi Isoaho^{a,b,*}, Lauri Ikkala^b, Hannu Marttila^b, Jan Hjort^c, Timo Kumpula^d, Pasi Korpelainen^d, Aleksi Räsänen^a

^a Natural Resources Institute Finland (Luke), Paavo Havaksen tie 3, FI-90570, Oulu, Finland

^b Water, Energy and Environmental Engineering Research Unit, Faculty of Technology, University of Oulu, P.O. Box 4300, Oulu, Finland

^c Geography Research Unit, Faculty of Science, University of Oulu, P.O. Box 8000, Oulu, Finland

^d Department of Geographical and Historical Studies, Faculty of Social Sciences and Business Studies, University of Eastern Finland, P.O. Box 111, FI-80101, Joensuu, Finland

ARTICLE INFO

Keywords:

Remote sensing
Multispectral
Thermal
Peatland
Hydrology
Restoration

ABSTRACT

Peatlands have been degrading globally, which is increasing pressure on restoration measures and monitoring. New monitoring methods are needed because traditional methods are time-consuming, typically lack a spatial aspect, and are sometimes even impossible to execute in practice. Remote sensing has been implemented to monitor hydrological patterns and restoration impacts, but there is a lack of studies that combine multi-sensor ultra-high-resolution data to assess the spatial patterns of hydrology in peatlands. We combine optical, thermal, and topographic unmanned aerial vehicle data to spatially model the water table level (WTL) in unditched open peatlands in northern Finland suffering from adjacent drainage. We predict the WTL with a linear regression model with a moderate fit and accuracy ($R^2 = 0.69$, $RMSE = 3.85$ cm) and construct maps to assess the spatial success of restoration. We demonstrate that thermal-optical trapezoid-based wetness models and optical bands are strongly correlated with the WTL, but topography-based wetness indices do not. We suggest that the developed method could be used for quantitative restoration assessment, but before-after restoration imagery is required to verify our findings.

1. Introduction

Peatlands cover 2.8% of the earth's surface (Xu et al., 2018), with 80% of the global peatland area located in boreal regions (Leifeld and Menichetti, 2018; Xu et al., 2018). Approximately 11% of the global peatland area has degraded because of human impacts (Leifeld and Menichetti, 2018).

In the boreal zone, drainage, e.g. for forestry, is one of the main reasons for the deteriorated state of peatlands (Minkkinen et al., 2008). Artificial drainage lowers the water table, as the ditch network surrounding the peatland prevents surface and near-surface groundwater flow to the peatland area (Holden et al., 2006). The reduced water supply slows and even stops peat accumulation (Stivins et al., 2017), causes peat degradation (Whittington and Price, 2006; Itoh et al., 2017; Ikkala et al., 2021), and on forestry-drained sites, makes the conditions more suitable for forest vegetation (Laine et al., 2006). Additionally, drainage and the resulting decomposition of peat increase the concentrations of nitrogen and phosphorus in surface waters (Nieminen et al., 2017;

* Corresponding author. Natural Resources Institute Finland (Luke), Paavo Havaksen tie 3, FI-90570 Oulu, Finland.

E-mail address: aleksi.isoaho@luke.fi (A. Isoaho).

<https://doi.org/10.1016/j.rsase.2023.101059>

Received 8 June 2023; Received in revised form 10 August 2023; Accepted 11 September 2023

Available online 13 September 2023

2352-9385/© 2023 The Authors. Published by Elsevier B.V. This is an open access article under the CC BY license (<http://creativecommons.org/licenses/by/4.0/>).

Marttila et al., 2018) and produce greenhouse gas (GHG) emissions (Leifeld and Menichetti, 2018; Wilkinson et al., 2023). Peatland drainage also has catchment-scale impacts on hydrological responses such as baseflow conditions (Meriö et al., 2019).

The deteriorated state of peatlands has created pressure for their restoration. Traditionally, restoration has been done, for example, by damming and infilling ditches and drainage channels (Andersen et al., 2017). Recently, restoration has also been conducted by excavating ditches to direct waterflow routes to unditched peatland areas (Autio et al., 2018; Kareksela et al., 2021) suffering from adjacent upslope drainage (Sallinen et al., 2019). However, there is a need to develop methods to assess the success of water-directing ditches, as the restoration method has become more systematic only recently, and there is a lack of scientific knowledge regarding its efficiency.

Previously, the success of restoration has been assessed with field monitoring such as field visits and automated data loggers, which measure the water table level (WTL). The WTL has been used as an indicator for changes in hydrology because on drained sites, the aim is a higher wetness level, and the WTL is typically closer to its pristine-like counterpart after restoration (Jauhiainen et al., 2002; Armstrong et al., 2010; Haapalehto et al., 2011, 2014; Menberu et al., 2016). Additionally, the WTL is an important indicator because it has been estimated that for specific sites, a rise in the WTL could reduce the annual net warming impact of GHG emissions (Evans et al., 2021). However, point-based field monitoring measures hydrological changes only at the measurement point, and the spatial variability of the changes is usually unknown. Importantly, changes in the WTL are not necessarily similar across a larger peatland area, and spatial variability has been reported on some restored sites (Haapalehto et al., 2014). Finally, some peatlands are difficult to reach, making traditional monitoring impossible.

To upscale field inventories, remote sensing (RS) techniques have proved useful when monitoring hydrology in boreal peatlands (Ikkala, 2023). Recent advances and the widespread use of unmanned aerial vehicles (UAV) offer new opportunities to peatland studies. They provide ultra-high-resolution data that can be used to monitor and model onsite changes in boreal peatlands with high spatial heterogeneity (Rahman et al., 2017; Räsänen and Virtanen, 2019; Ikkala et al., 2022; Steenvoorden et al., 2023). UAVs enable the collection of multi-sensor data, including multispectral, thermal, and topographic datasets, and they can even be collected if the target area is unreachable on foot.

Optical and thermal data have been used in soil moisture monitoring, as the reflectance and land surface temperature (LST) are correlated with soil moisture content (Gao et al., 2013; Babaeian et al., 2019; Wigmore et al., 2019). Individual spectral bands seem to be related to hydrological patterns in peatland studies, and most success has been found in shortwave infrared (SWIR) and visible light (Kolari et al., 2022; Räsänen et al., 2022). Additionally, various spectral indices related to moisture or wetness have been used as a proxy for onsite wetness (Kalacska et al., 2018; Šimanasienė et al., 2019; Räsänen et al., 2022). Moreover, some vegetation spectral indices such as the normalised difference vegetation index (NDVI; Tucker, 1979) have been correlated with the WTL in some studies (Zhang et al., 2014; Šimanasienė et al., 2019), but the link between them is probably indirect, as they are sensitive to vegetation greenness and composition (McPartland et al., 2019). The most recent advances are trapezoid-based RS models such as the Optical TRapezoid Model (OPTRAM; Sadeghi et al., 2017) and the Temperature Vegetation Drought Index (TVDI; Sandholt et al., 2002), which seem to have a strong relationship with the WTL and soil moisture in boreal peatlands (Holidi et al., 2019; Burdun et al., 2020a, 2020b; Räsänen et al., 2022). These models are based on the interpretation of the pixel distribution between a vegetation index and thermal data (TVDI) or SWIR (OPTRAM).

Topography has also been used to assess changes in hydrology in peatlands. Traditionally, topographic data have been produced with light detection and ranging (LiDAR), but the Structure from Motion (SfM) process has recently emerged as a good alternative for constructing topographic models in open areas (Mlambo et al., 2017). Soil moisture patterns have been determined with e.g. the topographic wetness index (TWI; Beven and Kirkby, 1979), which have been found to be positively correlated with onsite wetness (Kempinen et al., 2018; Riihimäki et al., 2021; Ikkala et al., 2022). The index also has potential for peatland moisture, and e.g. Ikkala et al. (2022) implemented the TWI to before-after peatland restoration UAV SfM Digital Terrain Models (DTMs), finding differences in overall wetness caused by altered flow routes.

Overall, numerous RS approaches have been implemented to monitor hydrological patterns and restoration impacts on peatlands. However, there is a lack of studies that combine multi-sensor ultra-high-resolution data with multivariate statistical modelling. There is also a scientific gap in the impact of water-directing ditches as a restoration measure. We therefore constructed a regression model in which field-measured WTL was the dependent variable, and UAV-based multispectral, thermal, and topographical variables were independent variables. We ask the following research questions: (1) How accurately can the spatial patterns of boreal peatland WTL be detected with UAV data? (2) Which UAV variables have the strongest relationships with the WTL? (3) Can the functionality of the water-directing ditches be assessed with the regression model?

2. Methods

2.1. Study sites and field data

We studied three different drained but relatively wet minerotrophic aapa mires (Makkarasuo, Kurkineva, Vihtaneva) in North Ostrobothnia, Finland (Fig. 1). In Makkarasuo, there were four separate study sites, while the other two mires included one study site each. The average annual precipitation was 625, 612, and 624 mm, and the annual mean temperature was 2.1, 2.9, and 3.0 °C between 1991 and 2020 for Makkarasuo, Kurkineva, and Vihtaneva respectively, based on Finland's gridded daily climatology data (Aalto et al., 2016; Finnish Meteorological Institute, 2023).

The studied sites are surrounded by drainage ditches excavated between the 1960s and 1990s. Additionally, the sites have been restored with water-directing ditches with the aim of bringing water from ditched to unditched areas (Fig. 1). In Makkarasuo, some ditches directing water to the open peatland area were excavated during drainage in the 1980s and 1990s, but only some take water to

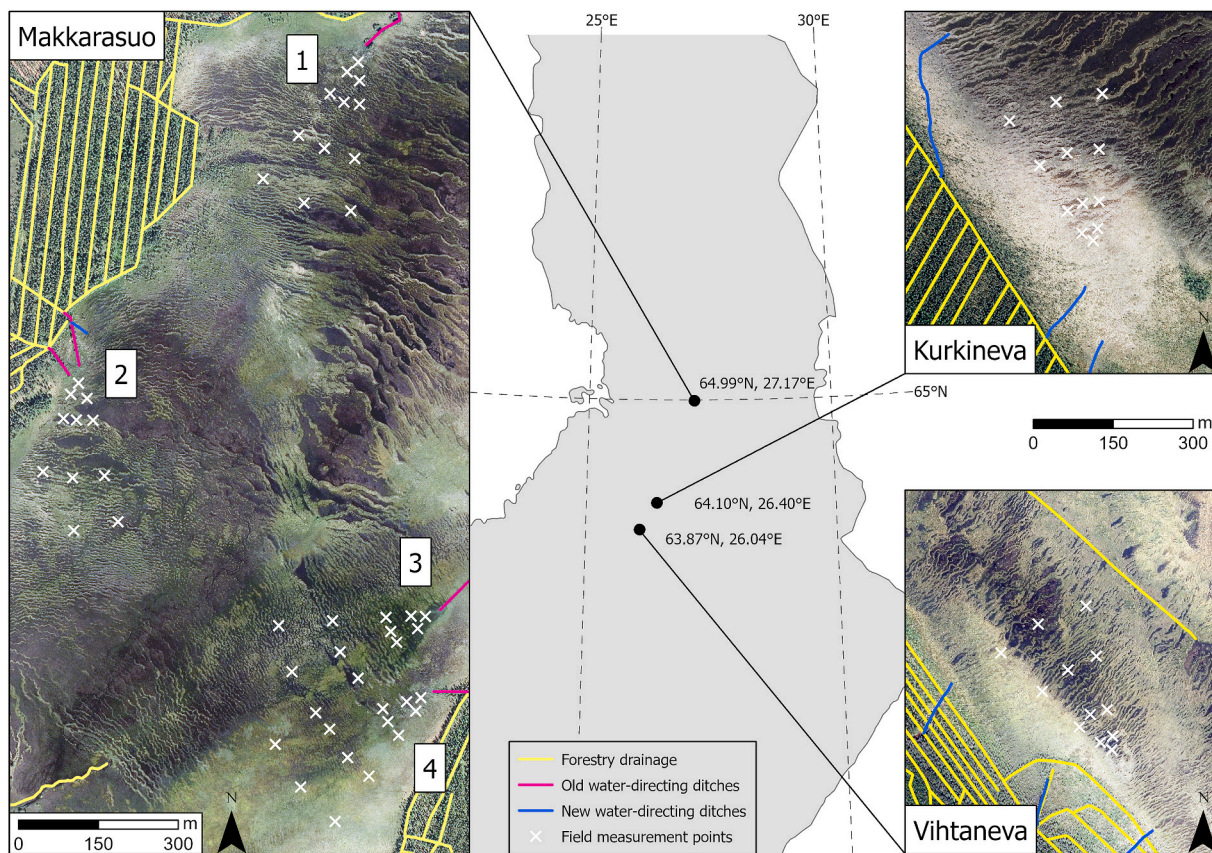


Fig. 1. The locations of the study sites and field measurements. Makkarasuo has four study sites, Kurkineva and Vihtaneva each have one. The old water-directing ditches were dug in the 1980s and 1990s, and the new water-directing ditches were dug in 2021. Vihtaneva's middle water-directing ditch is an enlargement of the old overgrown drainage ditch to which more water was directed in 2021. The aerial photos are open data from the National Land Survey of Finland.

Table 1

The minimum, median, and maximum value of the measured water table level per study site and as a total dataset.

Measured water table level (cm)	Makkarasuo1	Makkarasuo2	Makkarasuo34	Kurkineva	Vihtaneva	Total
Minimum	4	0	-7	-7	-4	-7
Median	10	9	7.5	-4.5	-1	4
Maximum	14	12	17	4	7	17
Number of measurements	12	11	24	12	12	71

the mire. Kurkineva and Vihtaneva were restored in the autumn of 2021 with new water-directing ditches. Moreover, in Makkarasuo2, a new water-directing ditch was excavated in the autumn of 2021, but it was left shorter than originally planned because the peatland surface did not support the excavator.

The studied sites have clear microtopographic patterns with alternating wet flarks and drier strings in elevated positions. Only a few Scots pines (*Pinus sylvestris*) and Norway spruce (*Picea abies*) grow close to the drained peatland margins, where the WTL is lower. The ground vegetation is characterised by abundant *Sphagnum* and wet brown moss cover. In the field layer, flarks are dominated by graminoids and some forbs, while there are also shrubs in the strings. According to the prevailing vegetation, Makkarasuo is more nutrient-rich than the other two studied peatlands and has more abundant herbaceous vegetation. Conversely, both Kurkineva and Vihtaneva have *Eriophorum vaginatum* coverage, which is largely absent in Makkarasuo.

The WTL was manually measured from perforated plastic standpipe wells drilled into the peatlands. The WTL was calculated relative to the peatland surface, so the level below was considered negative, and the level above positive. Twelve permanent standpipes were placed on each site in 2021 before the restoration measures, and their locations were measured with Real-time kinematic (RTK) positioning. They were placed in a fanlike shape, starting from the end of the planned or existing water-directing ditch. The measurement points were placed 25 m, 50 m, 100 m, 200 m, and 300 m away, with 1–3 pipes at each distance (Fig. 1). Because Makkarasuo3 and 4 were spatially very close, they were treated as one study site. One standpipe well in Makkarasuo2 was lost during the fieldwork, so the total number of WTL measurements was 71 (Table 1). The fieldwork was conducted on August 18, 2022 (Makkarasuo) and August 19, 2022 (Kurkineva and Vihtaneva).

2.2. UAV mapping and data pre-processing

We used a Matrice 300 RTK UAV with a MicaSense Altum-PT sensor to collect multispectral and thermal imagery. Altum-PT was radiometrically calibrated with reflectance panels and empirical line calibration. We also conducted RGB mapping with DJI Zenmuse

Table 2

Used remote sensing variables, abbreviations, equations, pixel sizes in imagery, data extraction methods, and number of pixels in extraction.

Type	Variable (and used bands/indices)	Abbreviation	Equation ^a	Pixel size (m)	Data extraction method	Number of pixels				
Optical	Blue reflectance	BLUE		0.051–0.056	0.25 m buffer	61–76				
	Green reflectance	GREEN								
	Red reflectance	RED								
	Red edge reflectance	RedEdge								
	Near-infrared reflectance	NIR								
	Normalised Difference Vegetation Index (RED, NIR)	NDVI	$\frac{NIR - RED}{NIR + RED}$							
	Normalised Difference Vegetation Index (GREEN, NIR)	NDWI	$\frac{GREEN - NIR}{GREEN + NIR}$							
	Normalised Difference Red Edge Index (RedEdge, NIR)	NDRE	$\frac{NIR - RedEdge}{NIR + RedEdge}$							
	Perpendicular Drought Index (RED, NIR)	PDI	$\frac{1}{\sqrt{M^2 + 1}}(RED + M \times NIR)$							
	Modified Perpendicular Drought Index (RED, NIR, NDVI)	MPDI	$\frac{RED + M \times NIR - f_v(RED_v + M \times NIR_v)}{(1 - f_v)\sqrt{M^2 + 1}}$							
	Optical/thermal	Temperature Vegetation Dryness Index (Land Surface Temperature, NDVI)	TVDI				$\frac{T_s - T_{smin}}{a + bNDVI - T_{smin}}$	0.316–0.343	1 m buffer	23–33
	Topographic	SAGA Wetness Index	SWI				$\ln\left(\frac{A_{SM}}{\tan \beta}\right)$	1	point	1
Depth to Water		DTW	$\left[\sum \frac{dz_i}{dx_i} a\right] x_c$							
Topographic Position Index		TPI	$z_0 - z$							

^a *M* is the soil line slope value; *f_v* is the vegetation fraction in a given pixel; *RED_v* and *NIR_v* are vegetation reflectance thresholds; *T_s* is the observed temperature in a given pixel; *T_{smin}* is the minimum surface temperature in a triangle (wet edge); *a* and *b* are the parameters defining the dry edge; *A_{SM}* is the modified catchment area; *β* is the slope angle; *dz_i/dx_i* is the slope of cell *i* along the least-cost path; *a* is 1 or 2^{0.5} when the path crosses the cell parallel to or diagonally across the grid; *x_c* is the grid cell size (m); *z₀* is the elevation in the grid cell; *z* is the average elevation within a predetermined area.

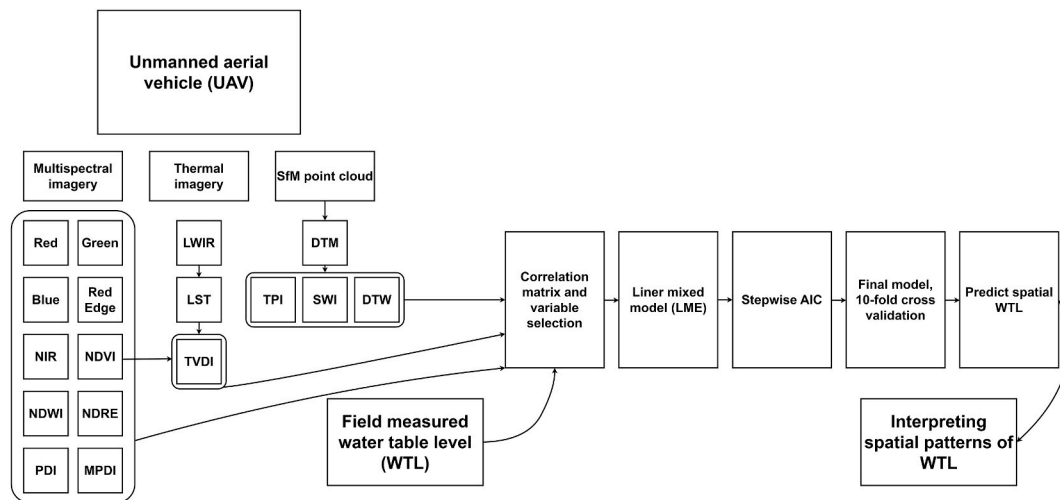


Fig. 2. Methodological flow chart. LWIR refers to long-wave infrared, LST refers to land surface temperature, DTM refers to digital terrain model, and SfM refers to Structure from Motion. The other abbreviations are explained in Table 2.

P1 and calculated point clouds with SfM processing in Agisoft Metashape (version 1.8.4) to obtain topographical RS data. The flights were carried out on August 15, 2022 (Kurkineva and Vihtaneva) and August 16, 2022 (Makkarasuo) in relatively cloudless and sunny weather.

To generate DTMs, we first removed duplicates from the SfM point clouds and then applied Statistical Outlier Removal (Rusu and Cousins, 2011) and Cloth Simulation Filter (Zhang et al., 2016) algorithms with parameter settings from Ikkala et al. (2022). We rasterised the filtered point clouds with the triangular irregular network (TIN) method with a resolution output of 1 m. UAV data pre-processing was done in R (version 4.2.1) with the *lidR* (Roussel et al., 2020) and *RCSF* (Roussel and Qi, 2020) packages.

2.3. Processing spectral and topographical data

Altum-PT collects information about the following spectral bands: blue; green; red; red edge; near-infrared (NIR); panchromatic; and long-wave infrared (LWIR). The digital numbers of the multispectral imagery were UInt-16 datatype. As the data were calibrated radiometrically, the land surface temperature (LST) from LWIR could be extracted with the formula presented on the MicaSense website (MicaSense, 2022).

We calculated the normalised difference water index (NDWI; McFeeters, 1996), NDVI, and the normalised difference red edge index (NDRE; Barnes et al., 2000) from the multispectral bands (Table 2). Moreover, we calculated three different pixel distribution models from the imagery: the TVDI; the perpendicular drought index (PDI); and the modified perpendicular drought index (MPDI) (Table 2). The PDI is based on pixel distribution between NIR and red reflection (Ghulam et al., 2007b), and the MPDI is a modified PDI which takes vegetation into account with the vegetation fraction parameter (Ghulam et al., 2007a). Both indices have been shown to be strongly correlated with soil moisture close to the surface outside peatlands (Zhang et al., 2015; Nie et al., 2020).

We parameterised the pixel distribution models visually because it has been suggested that visually inspected pixel distribution for triangle-based parametrisation is better than using mathematical solutions (Carlson, 2013; Sadeghi et al., 2017; Burdun et al., 2020b). The TVDI was calculated with unique wet and dry edge parameters for each site. In the PDI and MPDI, the relationship between red and NIR reflections behaved very similarly between the study sites, and we used the same soil line slope value universally. The vegetation fraction of the MPDI was calculated following the methodology of Baret et al. (1995) with the NDVI. We empirically determined the minimum (0.2) and maximum (1.0) values for the vegetation fraction based on the NDVI values in the bare soil and heavily vegetated areas of the study sites. The vegetation reflectance threshold values have been determined to be 0.05 and 0.5 for red reflection and NIR respectively in some previous studies (Ghulam et al., 2007a; Zhang et al., 2015). However, Gao et al. (2013) proposed that vegetation thresholds should be assessed based on the study area's reflections. Based on their methodology, we determined 0.03 and 0.4 for red reflection and NIR respectively, as these proved more effective in our initial tests.

We also produced three indices from SfM-based DTMs (Table 2). We calculated the SAGA Wetness Index (SWI; Böhner and Selige, 2006) which predicts relative wetness in flat areas more realistically than the original TWI (Western et al., 1999; Mattivi et al., 2019). The SWIs were constructed following the methodology of Ikkala et al. (2022), with the exception that the whole upper catchments were not included in the calculations, and 3×3 cell median filters were applied to the outputs to remove noise. In addition, we calculated the depth to water (DTW; Murphy et al., 2007) from the stream networks produced by the SAGA flow algorithm, with a threshold of 1000 m^2 and the topographic position index (TPI; Guisan et al., 1999; Weiss, 2001), with a $5 \times 5 \text{ m}$ rectangular area.

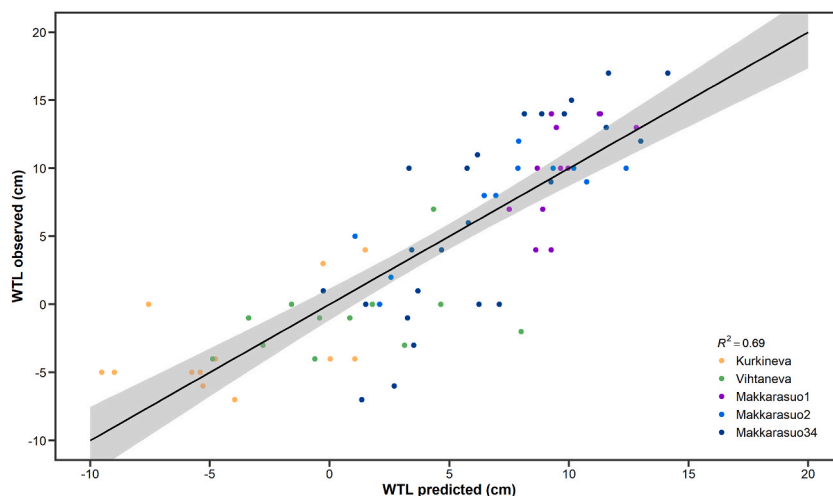


Fig. 3. Scatterplot between predicted and observed water table levels. The black line is the regression line between predictions and observations; the grey area is the 95% confidence interval for the regression. WTL refers to water table level.

Table 3

Results of the model's statistical analyses.

Analysed model		R^2	RMSE (cm)
Final model		0.69	3.85
10-fold cross-validation		0.72	3.94
Statistic of the final model	TVDI	RED	NDWI
Coefficient	-18.9225	-0.00818	25.129674
Standardised beta coefficient	-0.479	-0.403	0.141
Variance inflation factor	2.04	1.95	1.13

We tabulated data from spectral and topographical raster layers within the RTK-measured location of the field measurement points. To remove noise in multispectral variables, we applied a 0.25 m radius buffer around each field point and calculated the mean value from multispectral bands and indices within the buffered area. For the TVDI, we applied a 1 m buffer because of the larger pixel size of the LWIR band. For the topographical variables, we delivered raster values from specific pixels on the measurement points because of the large, 1 m, pixel size.

2.4. Statistical analyses

We used a linear mixed model (LME) to model the WTL and its spatial variation (Fig. 2) with RS variables and included the study site as a random effect factor. Highly cross-correlated explanatory variables (Spearman correlation coefficient $|r| > 0.7$) were excluded before the model was fitted. We also conducted a Spearman correlation analysis to check which variables had the strongest relationships with the WTL.

For the fitted model, we applied a backward and forward stepwise procedure by minimising Akaike's information criteria (AIC) value. To double-check the lack of multicollinearity, we calculated Variance Inflation Factor (VIF) values for the final model.

To assess the model's performance, we calculated the coefficient of the determination (R^2) and root mean square error (RMSE) and separately validated the model with 10-fold cross-validation. We also calculated standardised beta coefficients for the created model to assess the relative importance of selected variables. We conducted the analyses in R with the packages *nlme* (Pinheiro and Bates, 2000), *MuMIn* (Burnham and Anderson, 2004), *caret* (Kuhn, 2008), *MASS* (Venables et al., 2002), and *QuantPsyc* (Fletcher, 2022).

We predicted the WTL spatially with the constructed model and visually interpreted the model's performance based on empirical field experiences and orthophotos. In the spatial prediction, we resampled the explanatory variables to a resolution of 1 m with a bilinear interpolation method and delimited processing boundaries to an open peatland area.

3. Results

3.1. Regression model performance and spatial patterns of the WTL

The final model (Fig. 3) explained 69% of the WTL variance and had an RMSE of 3.85 cm. 10-fold cross-validation produced R^2 and RMSE that were almost equal to the full model (Table 3). The final model included the following variables: TVDI, RED, and NDWI. Based on standardised beta coefficients, the TVDI had the strongest effect, followed by RED, whereas the NDWI had the weakest effect (Table 3). The study site had no effect on the model performance, as marginal R^2 and conditional R^2 were the same.

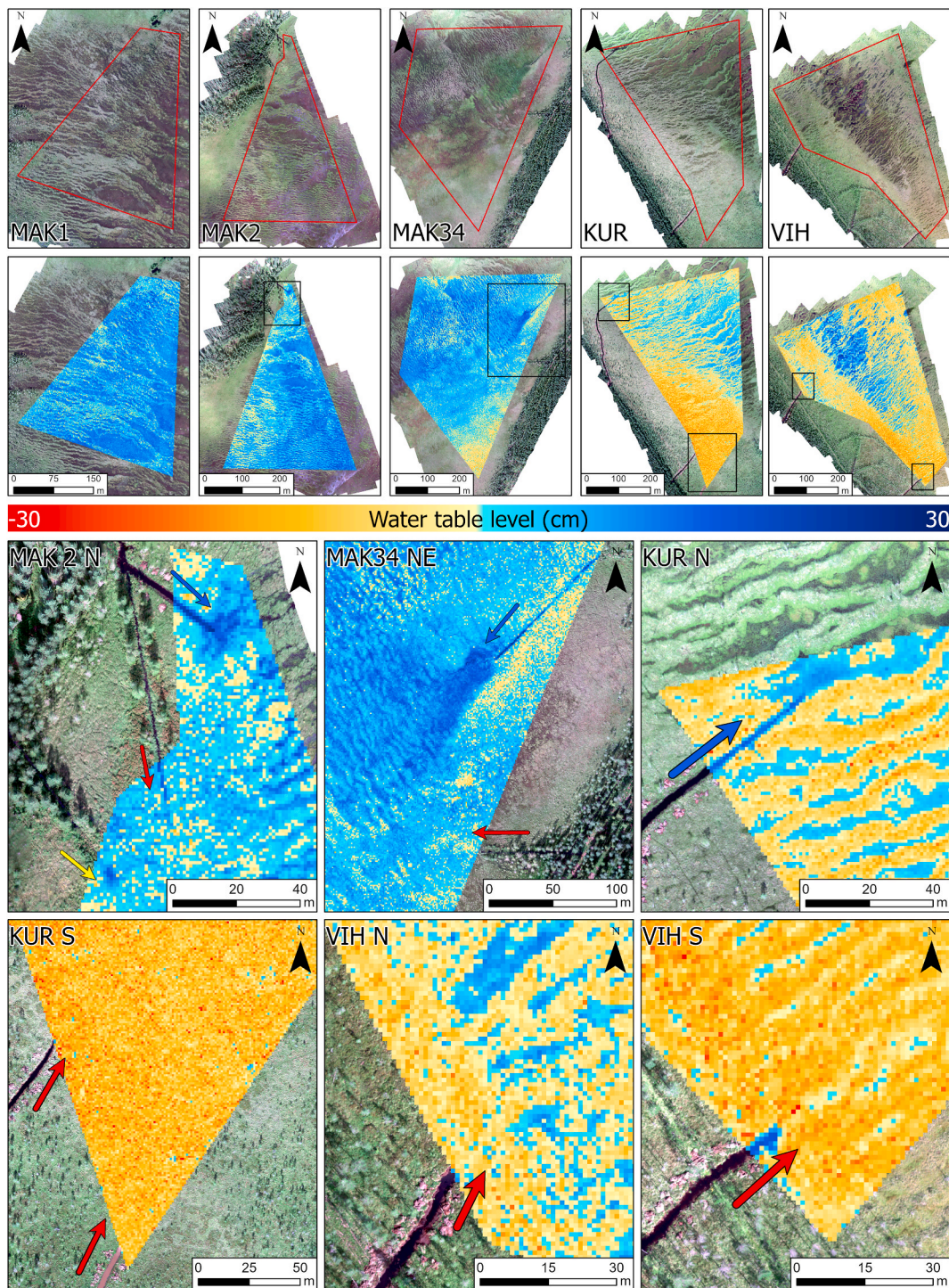


Fig. 4. Predicted water table level in Makkarasuo1 (MAK1), Makkarasuo2 (MAK2), Makkarasuo34 (MAK34), Kurkineva (KUR), and Vihtaneva (VIH). Below, the insets show the surroundings of the water-directing ditches, with the letters referring to North (N), East (E), and South (S). The coloured arrows indicate ditch functionality, with blue effective, yellow uncertain, and red not effective. The background orthophotos are RGB presentations of multispectral images taken in UAV campaigns with MicaSense Altum-PT. (For interpretation of the references to colour in this figure legend, the reader is referred to the Web version of this article.)

The spatial patterns of the predicted WTL were mostly plausible (Fig. 4). In Makkarasuo, the WTL was predicted to be mostly positive, which concurs with field observations, and the dense vegetation above the water did not hamper the model’s performance. At Kurkineva and Vihtaneva, the model seemed to slightly underestimate the WTL in flarks and overestimate the dryness in the driest

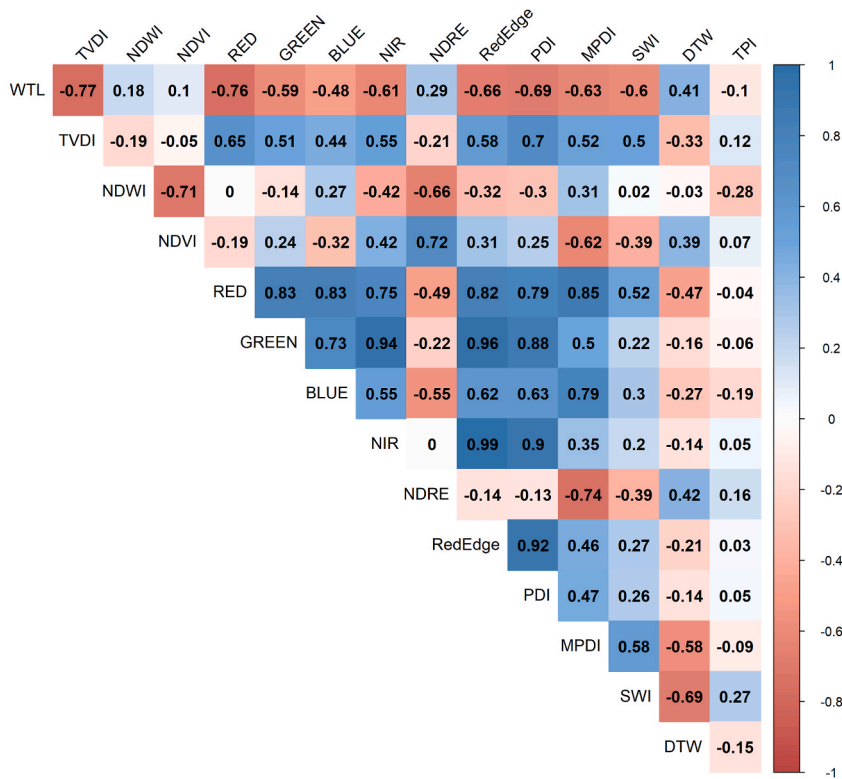


Fig. 5. Spearman's rank correlation coefficients between studied variables. WTL refers to water table level. The other abbreviations are explained in Table 2.

parts (Fig. 4).

3.2. Relationships between UAV variables and the WTL

Based on the correlation analysis, the highest correlation ($r = -0.77$) with the WTL was found for the TVDI (Fig. 5). Multispectral bands were moderately correlated with the WTL, with RED having the strongest correlation ($r = -0.76$). From the multispectral indices, the PDI and the MPDI had the strongest correlations ($r = -0.69, -0.63$) while the NDVI, the NDWI, and the NDRE had weak correlations ($|r| < 0.3$). For the topographical indices, the SWI was moderately correlated, and DTW was weakly correlated with the WTL, while the TPI had almost no correlation with any other variable. Because the SWI and DTW were correlated against expectations, and the TPI had almost no correlation, topographical indices were not included in the final model building.

3.3. Functionality of water-directing ditches

The functionality of the water-directing ditches, i.e. if they increased the WTL near the ditch endpoints, concurred with field observations (Fig. 4). In Makkarasuo34, the WTL was higher in the areas near the endpoint of the old northern ditch, while the eastern ditch did not affect the WTL. In Makkarasuo2, a new ditch from 2021 brought some water to the peatland, while the older ditches in the south appeared not to function properly (Fig. 4). In Kurkineva, the northern ditch seemed to work (Fig. 4), but the southern ditches were not supplying water, which also applied to the ditches on the Vihtaneva site (Fig. 4).

4. Discussion

4.1. Modelling the spatial patterns of the water table level

We showed that the spatial patterns of the WTL could be predicted with thermal-multispectral UAV data and a simple linear regression with moderate accuracy (Table 3, Fig. 3). This indicates that complex models with multiple explanatory variables are not mandatory in WTL prediction in boreal peatlands. This result is in line with e.g. Harris and Bryant (2009) and Burdun et al. (2020b), as they also found that utilising only a few RS variables could produce a well fitted model. However, Räsänen et al. (2022) highlighted the peatland type and site specificity of the functioning RS variables, as in their research, depending on the site, different bands and indices were the most important for predicting the WTL in a machine learning approach.

Maps for predicted hydrological variables have previously been made with RS approaches (Wigmore et al., 2019; Lendziocch et al., 2021), but to our knowledge, we have produced one of the first high-resolution peatland WTL maps with reasonable modelling accuracy. Alternatively, WTL and wetness patterns can also be visually and qualitatively interpreted straight from thermal imagery data, but our approach enables the quantitative spatial assessment of the WTL.

Our model seemed to underestimate high WTL in flarks (Fig. 3). The lack of field-measured extreme values probably decreased the model performance and increased the uncertainty in extreme value predictions. We did not conduct field measurements in the middle of the flarks, as they were inaccessible.

The optical RS bands had multicollinearity (Fig. 5), which has been reported multiple times (Nichol and Sarker, 2011; Chen et al., 2013; Li et al., 2014). We utilised only the best correlated variables in the model. In this process, some spectral information was lost. Principal component analysis could be utilised in these situations, as the derived components preserve a large proportion of spectral information from all bands. It could therefore improve prediction performance and be used as a solution for multicollinearity (Lafi and Kaneene, 1992; Zhao et al., 2020).

4.2. The usability of different UAV-based variables

Our results reinforce previous findings that the TVDI functions well in peatland soil moisture monitoring (Klinke et al., 2018; Wigmore et al., 2019). As the TVDI rescales the original thermal data and makes it more comparable with different sites and LSTs, it can be potentially used universally with different sites. It has also been reported that trapezoid models are not sensitive to parametrisation (Sadeghi et al., 2017), which eases the calculation of the index, as visual parametrisation functions well. However, the index is not necessarily an all-encompassing solution. There may be problems with imagery taken at different times of the growing season, as it has been suggested that northern latitude energy limitation violates the index assumption that lower soil moisture leads to an increase in the LST (Burdun et al., 2020a). Our study took place just after the peak of the thermic summer, in which it is assumed the assumption is met.

Red reflection has previously been observed to be strongly correlated with the wet flark area extent (Kolari et al., 2022), and our findings support this idea. Red outperformed all other spectral bands and multispectral indices. Moreover, in line with Kolar et al. (2022), spectral bands had a stronger correlation than most of the calculated spectral indices (Fig. 5). Only pixel distribution models outperformed all bands other than red. Based on previous studies (Ghulam et al., 2007a; Nie et al., 2020), the MPDI should perform better than the PDI in vegetated areas because the latter does not take the effect of vegetation into account, but this is not the case in our study. Previously, both indices have been calculated for coarser resolution satellite imagery, in which pixels cover very heterogeneous areas (Ghulam et al., 2007a; Nie et al., 2020), and as our UAV imagery pixels covered an area of a few centimetres, this could cause problems for parameterisation and the functionality of the indices. Additionally, our imagery was taken in very similar weather conditions which made the spectral bands from different sites very comparable. In more varying conditions, the pixel distribution indices could perform better than reflection bands.

Contrary to expectations, the SWI was negatively correlated with the WTL, contrary to what has been suggested in previous studies modelling soil moisture (Kemppinen et al., 2018; Riihimäki et al., 2021; Ikkala et al., 2022). As soil moisture is typically very strongly correlated with the WTL in peatlands (Lafleur et al., 2005; Strack and Price, 2009; Irfan et al., 2020), the measured variable is probably not the reason for the result. There are several possible reasons for the negative correlation. First, the SWI can be very sensitive to small changes in microtopography, and it is very difficult to estimate relative topographic wetness in small and flat peatland areas. Ikkala et al. (2022) also showed that most changes in the SWIs of pristine peatlands occurred in flat areas, where the index was most sensitive to small errors in the DTMs. Second, a large proportion of the peatland waterflow happens below the surface (Morris et al., 2022), and part of the vertical moisture transfer occurs in capillary form, which cannot be modelled with DTMs. Third, unlike Ikkala et al. (2022), we did not include the whole upper catchment in the calculations, which may have caused a bias in the spatial patterns of local SWIs. We lacked SfM-based DTMs for the whole catchments, and merging the data with existing LiDAR-based DTMs did not function properly due to the spatially irregular 10–20 cm height difference between the datasets. However, based on our tests with LiDAR-based coarser DTMs, the bias was probably minor, as neither of the LiDAR-based DTMs functioned in WTL modelling. Fourth, the SfM-based DTM may not represent topography in areas with dense field-layer vegetation, even if it has been filtered with different algorithms. This rationale also applies to the DTWs, as they were calculated from the same stream networks as the SWIs.

4.3. Assessing the functionality of water-directing ditches

The produced maps can be used in a quantitative peatland restoration impact assessment. In this study, the spatial impact of the water-directing ditches could be assessed. Based on a visual interpretation of the result of the WTL maps, ditches that brought water directly to wet flark areas increased the WTL in larger areas beyond the flarks. This was especially visible in an old northern ditch in Makkarasuo34 (Fig. 4). However, it was difficult to assess whether the new ditches ending in drier areas in Kurkineva and Vihtaneva worked, as there were no notable spatial differences in WTL patterns near the endpoints of the ditches. They may have been directing water more deeply into the peat layer, and this may have been impossible to observe with thermal-multispectral UAV data. Additionally, some individual tree shadow pixels were predicted with a positive WTL, even though they were in a dry area near Kurkineva's southern ditches (Fig. 4). It is therefore difficult to judge if the developed method can be utilised in drier areas with a denser tree canopy. Similar results have been reported by Burdun et al. (2020b) and Räsänen et al. (2022).

4.4. Future work

We showed that our methodology has potential in spatial assessments of the peatland state and the success of restoration, but the study left multiple possible research areas for further development. Our study areas were relatively wet and treeless peatlands; the method should therefore be tested on other sites, including drier and treed sites. The developed method should be further tested in restoration impact assessment, in which the restoration has been conducted with traditional methods, and in which the before-after imagery is available. Additionally, satellite imagery could be utilised, as successful ditches affected larger areas, and changes might also be visible with coarser spatial resolutions.

As the UAV data did not include SWIR wavelengths, we did not study many previous successfully used SWIR-based RS indices (Harris and Bryant, 2009; Kalacska et al., 2018; Räsänen et al., 2022). We suggest that UAV-SWIR may have potential in WTL modelling in spatially heterogeneous boreal peatlands. Some UAV-SWIR implementations have already been used successfully with various scientific topics, including peatland wetness (Honkavaara et al., 2016; Arroyo-Mora et al., 2017; Jenal et al., 2019, 2020). In utilising topographic data, the beginning of the growing season may be more suitable because the vegetation is less dense. Additionally, UAV LiDAR could also be utilised for topographical analysis because laser pulses can partly bypass the vegetation canopy, which facilitates the construction of DTMs (Mlambo et al., 2017; Liao et al., 2021).

5. Conclusion

We tested the functionality of thermal, optical, and topographic UAV data in the spatial modelling of the WTL in open peatlands. We showed that a linear regression model with explanatory variables calculated from multispectral and thermal imagery had a moderate explanatory capacity. The spatial patterns of the WTL were predicted plausibly, yet the errors were relatively largest in the areas with extreme values. The most important RS variables for the WTL included the TVDI and red reflectance, followed by other optical variables, while topographic variables did not function in WTL estimation. Based on a visual interpretation, our result's WTL maps indicate whether a water-directing ditch (i.e. a restoration measure) increases the peatland WTL locally. We suggest that the developed method could be used for restoration impact assessments, but before-after imagery is still needed for impact quantification.

Author statement

Aleksi Isoaho: Conceptualization, Methodology, Validation, Formal analysis, Investigation, Writing - Original Draft, Visualization. **Lauri Ikkala:** Writing - Review & Editing, Supervision. **Hannu Marttila:** Writing - Review & Editing, Supervision. **Jan Hjort:** Writing - Review & Editing, Supervision. **Timo Kumpula:** Investigation. **Pasi Korpelainen:** Investigation. **Aleksi Räsänen:** Conceptualization, Investigation, Resources, Writing - Review & Editing, Supervision, Project administration, Funding acquisition.

Declaration of competing interest

The authors declare that they have no known competing financial interests or personal relationships that could have appeared to influence the work reported in this paper.

Data availability

Data will be made available on request.

Acknowledgements:

The research was funded by the Ministry of the Environment, Finland and Natural Resources Institute Finland (VN/28337/2021-YM-2, VN/14352/2022, 41007-00216200). We thank Antti Rätty for his advice regarding statistical analyses. We also thank two anonymous reviewers for their valuable comments and suggestions which helped us improve the quality of the manuscript.

References

- Aalto, J., Pirinen, P., Jylhä, K., 2016. New gridded daily climatology of Finland: Permutation-based uncertainty estimates and temporal trends in climate. *J. Geophys. Res. Atmospheres* 121, 3807–3823. <https://doi.org/10.1002/2015JD024651>.
- Andersen, R., Farrell, C., Graf, M., Muller, F., Calvar, E., Frankard, P., Caporn, S., Anderson, P., 2017. An overview of the progress and challenges of peatland restoration in Western Europe: peatland restoration in Western Europe. *Restor. Ecol.* 25, 271–282. <https://doi.org/10.1111/rec.12415>.
- Armstrong, A., Holden, J., Kay, P., Francis, B., Foulger, M., Gledhill, S., McDonald, A.T., Walker, A., 2010. The impact of peatland drain-blocking on dissolved organic carbon loss and discolouration of water; results from a national survey. *J. Hydrol.* 381, 112–120. <https://doi.org/10.1016/j.jhydrol.2009.11.031>.
- Arroyo-Mora, J.P., Kalacska, M., Lucanus, O., Soffer, R.J., Leblanc, G., 2017. Spectro-spatial relationship between UAV derived high resolution DEM and SWIR hyperspectral data: application to an ombrotrophic peatland. In: Neale, C.M., Maltese, A. (Eds.), *Remote Sensing for Agriculture, Ecosystems, and Hydrology XIX*. Presented at the Remote Sensing for Agriculture, Ecosystems, and Hydrology. SPIE, Warsaw, Poland, p. 25. <https://doi.org/10.1117/12.2277874>.
- Autio, O., Jämsén, J., Rinkineva-Kantola, L., Joensuu, S., 2018. Veden Palauttamisen Kuivuneille Suojeluosille Kunnostusojituksen Yhteydessä (No. 10/2018), Raportteja. Etelä-Pohjanmaan ELY-Keskus.
- Babaeian, E., Sadeghi, M., Jones, S.B., Montzka, C., Vereecken, H., Tuller, M., 2019. Ground, Proximal, and satellite remote sensing of soil moisture. *Rev. Geophys.* 57, 530–616. <https://doi.org/10.1029/2018RG000618>.
- Baret, F., Clevers, J.G.P.W., Steven, M.D., 1995. The robustness of canopy gap fraction estimates from red and near-infrared reflectances: a comparison of approaches. *Remote Sens. Environ.* 54, 141–151. [https://doi.org/10.1016/0034-4257\(95\)00136-0](https://doi.org/10.1016/0034-4257(95)00136-0).
- Barnes, E.M., Clarke, T.R., Richards, S.E., Colaizzi, P.D., Haberland, J., Kostrzewski, M., Waller, P., Choi, C., Riley, E., Thompson, T., Lascano, R.J., Li, H., Moran, M.S., 2000. Coincident Detection of Crop Water Stress, Nitrogen Status and Canopy Density Using Ground-Based Multispectral Data. Presented at the Proceedings of the 5th International Conference on Precision Agriculture, Bloomington, Minnesota, USA.
- Beven, K.J., Kirkby, M.J., 1979. A physically based, variable contributing area model of basin hydrology/Un modèle à base physique de zone d'appel variable de l'hydrologie du bassin versant. *Hydrol. Sci. Bull.* 24, 43–69. <https://doi.org/10.1080/02626667909491834>.
- Böhner, J., Selige, T., 2006. Spatial prediction of soil attributes using terrain analysis and climate regionalisation. In: Böhner, J., McCloy, K., Strobl, J. (Eds.), *SAGA-analyses and Modelling Applications*. Göttinger Geographische Abhandlungen 115. Goltze.
- Burdun, I., Bechtold, M., Sagris, V., Komisarenko, V., De Lannoy, G., Mander, Ü., 2020a. A comparison of three trapezoid models using optical and thermal satellite imagery for water table depth monitoring in Estonian Bogs. *Rem. Sens.* 12. <https://doi.org/10.3390/rs12121980>, 1980.
- Burdun, I., Bechtold, M., Sagris, V., Lohila, A., Humphreys, E., Desai, A.R., Nilsson, M.B., De Lannoy, G., Mander, Ü., 2020b. Satellite determination of peatland water table temporal dynamics by localizing representative pixels of a SWIR-based moisture index. *Rem. Sens.* 12, 2936. <https://doi.org/10.3390/rs12182936>.
- Burnham, K.P., Anderson, D.R. (Eds.), 2004. *Model Selection and Multimodel Inference*. Springer New York, New York, NY. <https://doi.org/10.1007/b97636>.

- Carlson, T.N., 2013. Triangle models and misconceptions. *Int. J. Remote Sens. Appl.* 3.
- Chen, J., Quan, W., Wen, Z., Cui, T., 2013. A simple 'clear water' atmospheric correction algorithm for Landsat-5 sensors. I: a spectral slope-based method. *Int. J. Rem. Sens.* 34, 3787–3802. <https://doi.org/10.1080/01431161.2012.761740>.
- Evans, C.D., Peacock, M., Baird, A.J., Artz, R.R.E., Burden, A., Callaghan, N., Chapman, P.J., Cooper, H.M., Coyle, M., Craig, E., Cumming, A., Dixon, S., Gauci, V., Grayson, R.P., Helfter, C., Heppell, C.M., Holden, J., Jones, D.L., Kaduk, J., Levy, P., Matthews, R., McNamara, N.P., Misselbrook, T., Oakley, S., Page, S.E., Rayment, M., Ridley, L.M., Stanley, K.M., Williamson, J.L., Worrall, F., Morrison, R., 2021. Overriding water table control on managed peatland greenhouse gas emissions. *Nature* 593, 548–552. <https://doi.org/10.1038/s41586-021-03523-1>.
- Finnish Meteorological Institute, 2023. Daily Observations in 1km*1km Grid.
- Fletcher, T., 2022. Quantitative Psychology Tools.
- Gao, Z., Xu, X., Wang, J., Yang, H., Huang, W., Feng, H., 2013. A method of estimating soil moisture based on the linear decomposition of mixture pixels. *Math. Comput. Model.* 58, 606–613. <https://doi.org/10.1016/j.mcm.2011.10.054>.
- Ghulam, A., Qin, Q., Teyip, T., Li, Z.-L., 2007a. Modified perpendicular drought index (MPDI): a real-time drought monitoring method. *ISPRS J. Photogrammetry Remote Sens.* 62, 150–164. <https://doi.org/10.1016/j.isprsjprs.2007.03.002>.
- Ghulam, A., Qin, Q., Zhan, Z., 2007b. Designing of the perpendicular drought index. *Environ. Geol.* 52, 1045–1052. <https://doi.org/10.1007/s00254-006-0544-2>.
- Guisan, A., Weiss, S.B., Weiss, A.D., 1999. GLM versus CCA spatial modeling of plant species distribution. *Plant Ecol.* 1.
- Haapalahto, T., Kotiaho, J.S., Matilainen, R., Tahvanainen, T., 2014. The effects of long-term drainage and subsequent restoration on water table level and pore water chemistry in boreal peatlands. *J. Hydrol.* 519, 1493–1505. <https://doi.org/10.1016/j.jhydrol.2014.09.013>.
- Haapalahto, T., Vasander, H., Jauhiainen, S., Tahvanainen, T., Kotiaho, J.S., 2011. The effects of peatland restoration on water-table depth, elemental concentrations, and vegetation: 10 Years of changes. *Restor. Ecol.* 19, 587–598. <https://doi.org/10.1111/j.1526-100X.2010.00704.x>.
- Harris, A., Bryant, R.G., 2009. A multi-scale remote sensing approach for monitoring northern peatland hydrology: Present possibilities and future challenges. *J. Environ. Manag.* 90, 2178–2188. <https://doi.org/10.1016/j.jenvman.2007.06.025>.
- Holden, J., Evans, M.G., Burt, T.P., Horton, M., 2006. Impact of land drainage on peatland hydrology. *J. Environ. Qual.* 35, 1764–1778. <https://doi.org/10.2134/jeq2005.0477>.
- Holidi, H., Armanto, M.E., Damiri, N., Dwi Anugerah Putranto, D., 2019. Characteristics of selected peatland uses and soil moisture based on TVDI. *J. Ecol. Eng.* 20, 194–200. <https://doi.org/10.12911/22998993/102987>.
- Honkavaara, E., Eskelinen, M.A., Polonen, I., Saari, H., Ojanen, H., Mannila, R., Holmlund, C., Hakala, T., Litkey, P., Rosnell, T., Viljanen, N., Pulkkanen, M., 2016. Remote sensing of 3-D geometry and surface moisture of a peat Production area using hyperspectral frame cameras in visible to short-wave infrared spectral ranges onboard a small Unmanned Airborne Vehicle (UAV). *IEEE Trans. Geosci. Rem. Sens.* 54, 5440–5454. <https://doi.org/10.1109/TGRS.2016.2565471>.
- Ikkala, L., 2023. Airborne Remote Sensing as a Tool for Monitoring Topographical and Hydrological Changes on Northern Degraded and Restored Peatlands (Doctoral Dissertation). University of Oulu.
- Ikkala, L., Ronkanen, A.-K., Ilmonen, J., Similä, M., Rehell, S., Kumpula, T., Pääkkilä, L., Kløve, B., Marttila, H., 2022. Unmanned aircraft system (UAS) structure-from-motion (SfM) for monitoring the changed flow paths and wetness in minerotrophic peatland restoration. *Rem. Sens.* 14, 3169. <https://doi.org/10.3390/rs14133169>.
- Ikkala, L., Ronkanen, A.-K., Utriainen, O., Kløve, B., Marttila, H., 2021. Peatland subsidence enhances cultivated lowland flood risk. *Soil Tillage Res.* 212, 105078. <https://doi.org/10.1016/j.still.2021.105078>.
- Irfan, M., Kurniawati, N., Ariani, M., Sulaiman, A., Iskandar, I., 2020. Study of groundwater level and its correlation to soil moisture on peatlands in South Sumatra. *J. Phys. Conf. Ser.* 1568, 012028. <https://doi.org/10.1088/1742-6596/1568/1/012028>.
- Itoh, M., Okimoto, Y., Hirano, T., Kusin, K., 2017. Factors affecting oxidative peat decomposition due to land use in tropical peat swamp forests in Indonesia. *Sci. Total Environ.* 609, 906–915. <https://doi.org/10.1016/j.scitotenv.2017.07.132>.
- Jauhiainen, S., Laiho, R., Vasander, H., 2002. Ecohydrological and vegetational changes in a restored bog and fen. *Ann. Bot. Fenn.* 39.
- Jenal, A., Bareth, G., Bolten, A., Kneer, C., Weber, I., Bongartz, J., 2019. Development of a VNIR/SWIR multispectral imaging system for vegetation monitoring with unmanned aerial vehicles. *Sensors* 19, 5507. <https://doi.org/10.3390/s19245507>.
- Jenal, A., Lussem, U., Bolten, A., Gnyp, M.L., Schellberg, J., Jasper, J., Bongartz, J., Bareth, G., 2020. Investigating the potential of a newly developed UAV-based VNIR/SWIR imaging system for forage mass monitoring. *PFG – J. Photogramm. Remote Sens. Geoinformation Sci.* 88, 493–507. <https://doi.org/10.1007/s41064-020-00128-7>.
- Kalacska, M., Arroyo-Mora, J., Soffer, R., Roulet, N., Moore, T., Humphreys, E., Leblanc, G., Lucanus, O., Inamdar, D., 2018. Estimating peatland water table depth and net ecosystem exchange: a comparison between satellite and airborne imagery. *Rem. Sens.* 10, 687. <https://doi.org/10.3390/rs10050687>.
- Kareksela, S., Ojanen, P., Aapala, K., Haapalahto, T., Ilmonen, J., Koskinen, M., Laiho, R., Laine, A., Maanavilja, L., Marttila, H., Minkkinen, K., Nieminen, M., Ronkanen, A.-K., Sallantausta, T., Sarkkola, S., Tolvanen, A., Tuittila, E.-S., Vasander, H., 2021. Soiden ennallistamisen suoluento-, vesistö-, ja ilmastoaiheutukset. Vertaisarvioitu raportti. *Suom. Luontopaneelin Julk.* 2021/3b. <https://doi.org/10.17011/jyx/SLJ/2021/3b>.
- Kemppinen, J., Niittynen, P., Riihimäki, H., Luoto, M., 2018. Modelling soil moisture in a high-latitude landscape using LiDAR and soil data: soil moisture and LiDAR in a high-latitude landscape. *Earth Surf. Process. Landforms* 43, 1019–1031. <https://doi.org/10.1002/esp.4301>.
- Klinke, R., Kuechly, H., Frick, A., Förster, M., Schmidt, T., Holtgrave, A.-K., Kleinschmit, B., Spengler, D., Neumann, C., 2018. Indicator-based soil moisture monitoring of wetlands by utilizing sentinel and landsat remote sensing data. *PFG – J. Photogramm. Remote Sens. Geoinformation Sci.* 86, 71–84. <https://doi.org/10.1007/s41064-018-0044-5>.
- Kolari, T.H.M., Sallinen, A., Wolff, F., Kumpula, T., Tolonen, K., Tahvanainen, T., 2022. Ongoing fen–bog transition in a boreal aapa mire inferred from repeated field sampling, aerial images, and landsat data. *Ecosystems* 25, 1166–1188. <https://doi.org/10.1007/s10021-021-00708-7>.
- Kuhn, M., 2008. Building predictive models in R using the caret package. *J. Stat. Software* 28. <https://doi.org/10.18637/jss.v028.i05>.
- Lafi, S.Q., Kaneene, J.B., 1992. An explanation of the use of principal-components analysis to detect and correct for multicollinearity. *Prev. Vet. Med.* 13, 261–275. [https://doi.org/10.1016/0167-5877\(92\)90041-D](https://doi.org/10.1016/0167-5877(92)90041-D).
- Lafleur, P.M., Moore, T.R., Roulet, N.T., Frolking, S., 2005. Ecosystem respiration in a cool temperate bog depends on peat temperature but not water table. *Ecosystems* 8, 619–629. <https://doi.org/10.1007/s10021-003-0131-2>.
- Laine, J., Laiho, R., Minkkinen, K., Vasander, H., 2006. Forestry and boreal peatlands. In: Wielder, K., Vitt, D. (Eds.), *Boreal Peatland Ecosystems, Ecological Studies*. Springer Berlin, Heidelberg.
- Leifeld, J., Menichetti, L., 2018. The underappreciated potential of peatlands in global climate change mitigation strategies. *Nat. Commun.* 9, 1071. <https://doi.org/10.1038/s41467-018-03406-6>.
- Lendziach, T., Langhammer, J., Vlček, L., Minařík, R., 2021. Mapping the groundwater level and soil moisture of a montane peat bog using UAV monitoring and machine learning. *Rem. Sens.* 13, 907. <https://doi.org/10.3390/rs13050907>.
- Li, X., Zhang, Y., Bao, Y., Luo, J., Jin, X., Xu, X., Song, X., Yang, G., 2014. Exploring the best hyperspectral features for LAI estimation using Partial least squares regression. *Rem. Sens.* 6, 6221–6241. <https://doi.org/10.3390/rs6076221>.
- Liao, J., Zhou, J., Yang, W., 2021. Comparing LiDAR and SfM digital surface models for three land cover types. *Open Geosci.* 13, 497–504. <https://doi.org/10.1515/geo-2020-0257>.
- Marttila, H., Karjalainen, S.-M., Kuoppala, M., Nieminen, M.L., Ronkanen, A.-K., Kløve, B., Hellsten, S., 2018. Elevated nutrient concentrations in headwaters affected by drained peatland. *Sci. Total Environ.* 643, 1304–1313. <https://doi.org/10.1016/j.scitotenv.2018.06.278>.
- Mattivi, P., Franci, F., Lambertini, A., Bitelli, G., 2019. TWI computation: a comparison of different open source GISs. *Open Geospatial Data Softw. STAND* 4, 6. <https://doi.org/10.1186/s40965-019-0066-y>.
- McFeeters, S.K., 1996. The use of the Normalized Difference Water Index (NDWI) in the delineation of open water features. *Int. J. Rem. Sens.* 17, 1425–1432. <https://doi.org/10.1080/01431169608948714>.

- McPartland, M.Y., Kane, E.S., Falkowski, M.J., Kolka, R., Turetsky, M.R., Palik, B., Montgomery, R.A., 2019. The response of boreal peatland community composition and NDVI to hydrologic change, warming, and elevated carbon dioxide. *Global Change Biol.* 25, 93–107. <https://doi.org/10.1111/gcb.14465>.
- Menberu, M.W., Tahvanainen, T., Marttila, H., Irannezhad, M., Ronkanen, A.-K., Penttinen, J., Kløve, B., 2016. Water-table-dependent hydrological changes following peatland forestry drainage and restoration: analysis of restoration success. *Water Resour. Res.* 52, 3742–3760. <https://doi.org/10.1002/2015WR018578>.
- Meriö, L., Ala-aho, P., Linjama, J., Hjort, J., Kløve, B., Marttila, H., 2019. Snow to precipitation ratio controls catchment storage and summer flows in boreal headwater catchments. *Water Resour. Res.* 55, 4096–4109. <https://doi.org/10.1029/2018WR023031>.
- MicaSense, 2022. Altum and Altum-PT Thermal Band - FAQ.
- Minkkinen, K., Byrne, K., Trettin, C., 2008. Climate impacts of peatland forestry. In: Strack, M. (Ed.), *Peatlands and Climate Change*. International Peatland Society.
- Mlambo, R., Woodhouse, I., Gerard, F., Anderson, K., 2017. Structure from motion (SfM) Photogrammetry with drone data: a low cost method for monitoring greenhouse gas emissions from forests in developing countries. *Forests* 8, 68. <https://doi.org/10.3390/f8030068>.
- Morris, P.J., Davies, M.L., Baird, A.J., Balliston, N., Bourgault, M.-A., Clymo, R.S., Fewster, R.E., Furukawa, A.K., Holden, J., Kessel, E., Ketcheson, S.J., Kløve, B., Larocque, M., Marttila, H., Menberu, M.W., Moore, P.A., Price, J.S., Ronkanen, A.-K., Rosa, E., Strack, M., Surridge, B.W.J., Waddington, J.M., Whittington, P., Wilkinson, S.L., 2022. Saturated hydraulic conductivity in northern peats inferred from other measurements. *Water Resour. Res.* 58 <https://doi.org/10.1029/2022WR033181>.
- Murphy, P.N.C., Ogilvie, J., Connor, K., Arp, P.A., 2007. Mapping wetlands: a comparison of two different approaches for New Brunswick, Canada. *Wetlands* 27, 846–854. [https://doi.org/10.1672/0277-5212\(2007\)27\[846:MWACOT\]2.0.CO;2](https://doi.org/10.1672/0277-5212(2007)27[846:MWACOT]2.0.CO;2).
- Nichol, J.E., Sarker, MdL.R., 2011. Improved biomass estimation using the texture parameters of two high-resolution optical sensors. *IEEE Trans. Geosci. Rem. Sens.* 49, 930–948. <https://doi.org/10.1109/TGRS.2010.2068574>.
- Nie, Y., Tan, Y., Deng, Y., Yu, J., 2020. Suitability evaluation of typical drought index in soil moisture retrieval and monitoring based on optical images. *Rem. Sens.* 12, 2587. <https://doi.org/10.3390/rs12162587>.
- Nieminen, M., Sallantausta, T., Ukonmaanaho, L., Nieminen, T.M., Sarkkola, S., 2017. Nitrogen and phosphorus concentrations in discharge from drained peatland forests are increasing. *Sci. Total Environ.* 609, 974–981. <https://doi.org/10.1016/j.scitotenv.2017.07.210>.
- Pinheiro, J.C., Bates, D.M., 2000. *Mixed-Effects Models in S and S-PLUS*. Springer International Publishing, Cham.
- Rahman, M.M., McDermid, G.J., Strack, M., Lovitt, J., 2017. A new method to map groundwater table in peatlands using unmanned aerial vehicles. *Rem. Sens.* 9, 1057. <https://doi.org/10.3390/rs9101057>.
- Räsänen, A., Tolvanen, A., Kareksela, S., 2022. Monitoring peatland water table depth with optical and radar satellite imagery. *Int. J. Appl. Earth Obs. Geoinformation* 112, 102866. <https://doi.org/10.1016/j.jag.2022.102866>.
- Räsänen, A., Virtanen, T., 2019. Data and resolution requirements in mapping vegetation in spatially heterogeneous landscapes. *Remote Sens. Environ.* 230, 111207 <https://doi.org/10.1016/j.rse.2019.05.026>.
- Riihimäki, H., Kempainen, J., Kopecký, M., Luoto, M., 2021. Topographic wetness index as a proxy for soil moisture: the importance of flow-routing algorithm and grid resolution. *Water Resour. Res.* 57 <https://doi.org/10.1029/2021WR029871>.
- Roussel, J.-R., Auty, D., Coops, N.C., Tompalski, P., Goodbody, T.R.H., Meador, A.S., Bourdon, J.-F., de Boissieu, F., Achim, A., 2020. lidR: an R package for analysis of Airborne Laser Scanning (ALS) data. *Remote Sens. Environ.* 251, 112061 <https://doi.org/10.1016/j.rse.2020.112061>.
- Roussel, J.-R., Qi, J., 2020. RCSF: Airborne LiDAR Filtering Method Based on Cloth Simulation.
- Rusu, R.B., Cousins, S., 2011. 3D is here: point cloud library (PCL). In: 2011 IEEE International Conference on Robotics and Automation. Presented at the 2011 IEEE International Conference on Robotics and Automation (ICRA). IEEE, Shanghai, China, pp. 1–4. <https://doi.org/10.1109/ICRA.2011.5980567>.
- Sadeghi, M., Babaeian, E., Tuller, M., Jones, S.B., 2017. The optical trapezoid model: a novel approach to remote sensing of soil moisture applied to Sentinel-2 and Landsat-8 observations. *Remote Sens. Environ.* 198, 52–68. <https://doi.org/10.1016/j.rse.2017.05.041>.
- Sallinen, A., Tuominen, S., Kumpula, T., Tahvanainen, T., 2019. Undrained peatland areas disturbed by surrounding drainage: a large scale GIS analysis in Finland with a special focus on aapa mires. *Mires Peat* 1–22. <https://doi.org/10.19189/Map.2018.AJB.391>.
- Sandholt, I., Rasmussen, K., Andersen, J., 2002. A simple interpretation of the surface temperature/vegetation index space for assessment of surface moisture status. *Remote Sens. Environ.* 79, 213–224. [https://doi.org/10.1016/S0034-4257\(01\)00274-7](https://doi.org/10.1016/S0034-4257(01)00274-7).
- Šimanauskienė, R., Linkevičienė, R., Bartold, M., Dąbrowska-Zielińska, K., Slavinskienė, G., Veteikiš, D., Taminskas, J., 2019. Peatland degradation: the relationship between raised bog hydrology and normalized difference vegetation index. *Ecohydrology* 12. <https://doi.org/10.1002/eco.2159>.
- Steenvoorden, J., Bartholomeus, H., Limpens, J., 2023. Less is more: optimizing vegetation mapping in peatlands using unmanned aerial vehicles (UAVs). *Int. J. Appl. Earth Obs. Geoinformation* 117, 103220. <https://doi.org/10.1016/j.jag.2023.103220>.
- Stivriņš, N., Ozola, I., Gaika, M., 2017. Drivers of peat accumulation rate in a raised bog: impact of drainage, climate, and local vegetation composition. *Mires Peat* 1–19. <https://doi.org/10.19189/Map.2016.OMB.262>.
- Strack, M., Price, J.S., 2009. Moisture controls on carbon dioxide dynamics of peat- *Sphagnum* monoliths. *Ecohydrology* 2, 34–41. <https://doi.org/10.1002/eco.36>.
- Tucker, C.J., 1979. Red and photographic infrared linear combinations for monitoring vegetation. *Remote Sens. Environ.* 8, 127–150. [https://doi.org/10.1016/0034-4257\(79\)90013-0](https://doi.org/10.1016/0034-4257(79)90013-0).
- Venables, W.N., Ripley, B.D., Venables, W.N., 2002. *Modern applied statistics with S*. In: *Statistics and Computing*, fourth ed. Springer, New York.
- Weiss, A.D., 2001. *Topographic Position and Landforms Analysis*.
- Western, A.W., Grayson, R.B., Blöschl, G., Willgoose, G.R., McMahon, T.A., 1999. Observed spatial organization of soil moisture and its relation to terrain indices. *Water Resour. Res.* 35, 797–810. <https://doi.org/10.1029/1998WR900065>.
- Whittington, P.N., Price, J.S., 2006. The effects of water table draw-down (as a surrogate for climate change) on the hydrology of a fen peatland. *Canada. Hydrol. Process.* 20, 3589–3600. <https://doi.org/10.1002/hyp.6376>.
- Wigmore, O., Mark, B., McKenzie, J., Baraer, M., Lautz, L., 2019. Sub-metre mapping of surface soil moisture in proglacial valleys of the tropical Andes using a multispectral unmanned aerial vehicle. *Remote Sens. Environ.* 222, 104–118. <https://doi.org/10.1016/j.rse.2018.12.024>.
- Wilkinson, S.L., Andersen, R., Moore, P.A., Davidson, S.J., Granath, G., Waddington, J.M., 2023. Wildfire and degradation accelerate northern peatland carbon release. *Nat. Clim. Change*. <https://doi.org/10.1038/s41558-023-01657-w>.
- Xu, J., Morris, P.J., Liu, J., Holden, J., 2018. PEATMAP: refining estimates of global peatland distribution based on a meta-analysis. *Catena* 160, 134–140. <https://doi.org/10.1016/j.catena.2017.09.010>.
- Zhang, J., Zhou, Z., Yao, F., Yang, L., Hao, C., 2015. Validating the modified perpendicular drought index in the North China region using in situ soil moisture measurement. *Geosci. Rem. Sens. Lett. IEEE* 12, 542–546. <https://doi.org/10.1109/LGRS.2014.2349957>.
- Zhang, W., Lu, Q., Song, K., Qin, G., Wang, Y., Wang, X., Li, Hongxia, Li, J., Liu, G., Li, Hua, 2014. Remotely sensing the ecological influences of ditches in Zoige Peatland, eastern Tibetan Plateau. *Int. J. Rem. Sens.* 35, 5186–5197. <https://doi.org/10.1080/01431161.2014.939779>.
- Zhang, W., Qi, J., Wan, P., Wang, H., Xie, D., Wang, X., Yan, G., 2016. An easy-to-use airborne LiDAR data filtering method based on Cloth simulation. *Rem. Sens.* 8, 501. <https://doi.org/10.3390/rs8060501>.
- Zhao, R., Zhan, L., Yao, M., Yang, L., 2020. A geographically weighted regression model augmented by Geodetector analysis and principal component analysis for the spatial distribution of PM2.5. *Sustain. Cities Soc.* 56, 102106 <https://doi.org/10.1016/j.scs.2020.102106>.